ELSEVIER

Journal of Photochemistry and Photobiology
A: Chemistry 86 (1995) 231–239

Journal of PHOTOCHEMISTRY AND PHOTOBIOLOGY A: CHEMISTRY

Photodecomposition of anthracene on dry surfaces: products and mechanism

Reza Dabestani *, Keith J. Ellis, Michael E. Sigman

Chemical and Analytical Sciences Division, Oak Ridge National Laboratory, P.O. Box 2008, Oak Ridge, TN 37831-6100, USA

Received 5 May 1994; accepted 9 August 1994

Abstract

The photochemistry of anthracene (**1**) was studied on dry surfaces of silica, Cab-O-Sil (fumed silica) and alumina (neutral) at low coverages (less than 11% of a monolayer). The adsorption of **1** onto these surfaces from cyclohexane obeys a Freundlich adsorption isotherm, demonstrating a distribution of adsorption sites for interactions between **1** and the surface. Photolysis of **1** (λ_{ex} = 350 nm) adsorbed on silica, Cab-O-Sil or alumina, under deaerated conditions, proceeds slowly to give the anthracene-9,10-photodimer (**2**) as the only product. Diffuse reflectance and fluorescence spectroscopy show that a novel process, involving the formation of a stable ground state pair between two molecules of **1** takes place on all three surfaces at coverages of more than 1% of a monolayer. We propose a dimerization mechanism involving a singlet excimer formed from the stable ground state pairs. Photolysis at the solid–air interface, on the other hand, is considerably faster and proceeds to give **2** and photo-oxidation products of **1**. The primary oxidation product is anthracene-9,10-endoperoxide (**3**) which undergoes thermal decomposition on the surface to give 9,10-anthraquinone (**4**), 9,10-dihydro-9,10-dihydroxyanthracene (**5**), bianthronyl (**6**), 9-hydroxyanthrone (**7**) and 10,10′-dihydroxy-9,9′,10,10′-tetrahydro-9,9′-bianthryl (**8**) as the secondary products. Photo-oxidation is mediated by the addition of singlet molecular oxygen to ground state **1**.

Keywords: Photodecomposition; Anthracene; Dimerization; Singlet excimer

1. Introduction

Polynuclear aromatic hydrocarbons (PAHs) comprise a large class of anthropogenic pollutants which are released into the environment as a result of the production and consumption of fossil fuels. Light-induced processes have been shown to play a key role in the transformation of these anthropogenic pollutants [1–3]. The adsorption of organic molecules at the solid–liquid interface is a crucial factor which can influence the transport of these pollutants in the environment [4,5]. Since the oxidation of PAHs at the solid–liquid and solid–air interfaces can have a significant impact in controlling their residence time in the environment, it is important to study their photochemistry under conditions which mimic natural environmental settings. The role of surface interactions (e.g. hydrogen bonding) on the photophysics and photochemistry of pyrene on different surfaces has been well documented [6–13]. Previous studies [14–16] designed to probe the chemistry at the solid–liquid [14] and solid–air [15,16] interfaces have revealed that highly polar surfaces, such as silica and alumina, exert a dramatic influence on the photoreactivity of a number of these PAHs. In our initial investigation of the photochemistry of **1** at an SiO_2–cyclohexane interface [14], we reported that **1** undergoes exclusively photo-oxidation in aerated slurries. In the present study, we have examined the photochemistry of **1** at the solid–air interface on a variety of surfaces. The objectives of this investigation were as follows: (a) to determine whether or not **1** undergoes photo-oxidation and/or photodimerization on different types of surface; (b) to identify the products and examine the role of the different surfaces on product distribution; (c) to determine the nature of the intermediates responsible for photodimerization and photo-oxidation (e.g. singlet oxygen and/or superoxide).

2. Experimental details

Anthracene (**1**) (scintillation grade, Reilly Tar & Chemicals Corporation) and anthracene-9,10-photodimer (**2**) (PCR Research Chemicals, Gainsville, FL)

* Corresponding author.

SSDI 1010-6030(94)03945-3

were used as received. 9,10-Anthraquinone (**4**) (Aldrich Chemical Company, Inc., Milwaukee, WI) and bianthronyl (**6**) (Sigma Chemical Company, St. Louis, MO) were recrystallized from toluene before use. Anthracene-9,10-endoperoxide (**3**), 9,10-dihydro-9,10-dihydroxyanthracene (**5**), 9-hydroxyanthrone (**7**) and 10,10′-dihydroxy-9,9′,10,10′-tetrahydro-9,9′-bianthryl (**8**) were synthesized by literature methods as reported previously [17]. Cyclohexane HPLC grade, Baker Analyzed, Phillipsburg, NJ) was dried over $MgSO_4$ and filtered before use. Acetonitrile (HPLC grade, Baxter Healthcare Corporation, Burdick and Jackson Division, Muskegon, MI), methanol (HPLC grade, Baker Analyzed, Phillipsburg, NJ), toluene (HPLC grade, Burdick and Jackson Laboratories Inc., Muskegon, MI) and methylene chloride (HPLC grade, Baker Analyzed, Phillipsburg, NJ) were used without further purification. Silica-60 (60–200 mesh, Baker Analyzed, Phillipsburg, NJ; N_2 Branauer–Emmett–Teller (BET) surface area, 340 m^2 g^{-1}; average pore diameter, 6 nm) was activated at 200 °C for at least 24 h before use. It had the following assay: Fe, less than 10 ppm; aluminum, 141.4 ppm; copper, less than 4.9 ppm. (Quantitative analysis was carried out at Galbraith Laboratories, Inc. Knoxville, TN.) Cab-O-Sil (Cabot Corporation, Tuscola, IL), an amorphous fumed silica with a BET surface area of 200 m^2 g^{-1}, and neutral alumina (50–200 mesh, Baker Analyzed with a BET surface area of 129 m^2 g^{-1}) were activated at 200 °C before use. The adsorption of **1** onto different surfaces was achieved by a cyclohexane slurry method as described previously [14,16]. The surface coverage (percentage of a monolayer) was calculated by fractal theory as described previously [14,16].

Samples (4 g) were photolyzed at 350 nm in uranium glass tubes (330 mm cut-off; outer diameter, 1 in) using a Rayonet RPR-208 photoreactor equipped with a merry-go-round attached in a horizontal configuration as described previously [15]. Photolysis products and unreacted **1** were extracted from the surface by multiple washing with methylene chloride, cyclohexane, methanol and acetonitrile to ensure complete removal of the materials from the surface. Solvents were then removed under vacuum at room temperature, and the residue was dissolved in a known volume of acetonitrile for quantitative HPLC analysis. Product analysis was carried out by reverse phase (C_{18}; column inner diameter, 2.1 mm) HPLC (Hewlett Packard model 1090), with a diode-array detector to record the UV–visible spectra of the eluting materials. All analyses were run isocratically at 75% acetonitrile and 25% H_2O with a flow rate of 0.21 ml min^{-1}. Calibration for quantitative HPLC analysis of the photoproducts was performed with authentic samples which were commercially available or synthesized (see above). The material balance was more than 90% of total **1** lost at low coverages.

Diffuse reflectance spectra were recorded on a Cary 4E UV–visible spectrophotometer (Varian) equipped with an integrating sphere. Fluorescence spectra were obtained on a Spex-Fluorolog-2 spectrometer equipped with double monochromators on both excitation and emission sides. Spectra were recorded from the front face of a cell containing the solid sample and were corrected for instrument response using correction factors provided by the manufacturer. All spectra were corrected for background using a corrected spectrum of the solid support which was not loaded with **1**. The cell was equipped with an Ace-Glass fitting to allow degassing and backfilling with oxygen-free nitrogen (Linde Gases, Knoxville, TN).

Singlet oxygen luminescence measurements were performed on a homebuilt IR spectrophotometer described previously [16]. Singlet oxygen emission from solid samples of **1** on silica and Cab-O-Sil was obtained using steady state irradiation ($\lambda_{ex} > 300$ nm) of 2.5×10^{-5} mol g^{-1} solid samples. The steady state emission spectrum of $^1O_2$ was recorded between 1200 and 1350 nm at a resolution of 2 nm (Fig. 7, see Section 3.2).

3. Results and discussion

The adsorption of **1** onto silica from cyclohexane has been shown to follow a modified Freundlich adsorption isotherm [14]. We have measured the adsorption of **1** onto Cab-O-Sil and neutral alumina from cyclohexane for a wide range of initial concentrations (1×10^{-5}–0.01 M for Cab-O-Sil and $1 \times 10^{-5} - 1 \times 10^{-3}$ M for alumina). For both surfaces, the data also adhere to a modified Freundlich adsorption isotherm. The intensity of adsorption decreases in the following order: alumina > silica ≈ Cab-O-Sil. For the concentration range studied, the equilibrium adsorption potentials, calculated as described previously [14], fall between 1.3 and 6.8 kcal mol^{-1} for alumina and 0.5 and 4 kcal mol^{-1} for both silica and Cab-O-Sil, indicating a stronger interaction between **1** and alumina compared with silica and Cab-O-Sil.

Fig. 1 shows the absorption spectrum of **1** in cyclohexane and the diffuse reflectance spectra of **1** on silica, alumina and Cab-O-Sil surfaces. On the surface, a new red-shifted band centered at around 390 nm is observed. This band is similar to that reported by Ferguson et al. [18–20] in rigid media for a ground state stable pair formed between two anthracene molecules. The configuration of this stable pair of **1** is such that the long axes are parallel and the planes of the two monomers are at 60° ± 15° [19]. Ford and Kamat [21] have also reported the formation of stable pairs for anthracene sulfonates on colloidal alumina-coated silica particles.

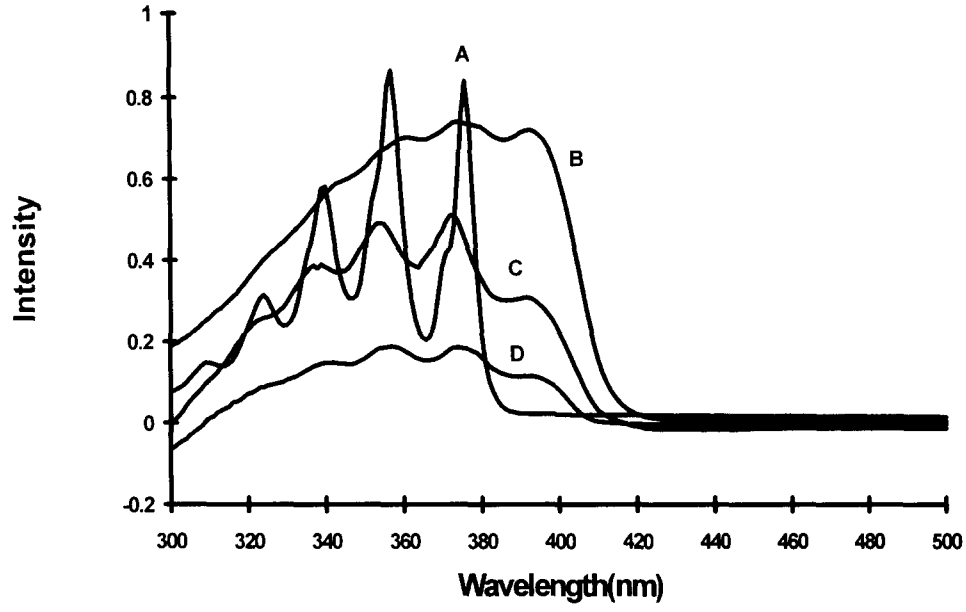

Fig. 1. Absorption spectrum of **1** in cyclohexane (A, 1×10^{-4} M) and diffuse reflectance spectra on neutral alumina (B, 2.7×10^{-5} mol g^{-1}, 7.2% of a monolayer), silica (C, 8.5×10^{-5} mol g^{-1}, 8.5% of a monolayer) and Cab-O-Sil (D, 3.1×10^{-5} mol g^{-1}, 5.3% of a monolayer).

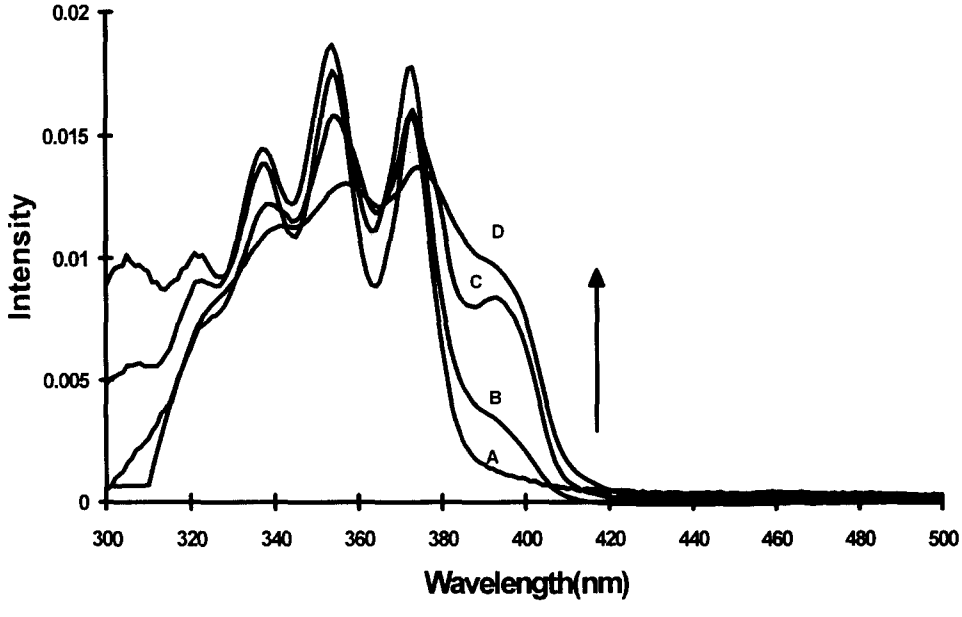

Fig. 2. Normalized diffuse reflectance spectra of **1** on dry silica for different coverages: A (0.5%), B (1.7%), C (3.2%) and D (8.8% of a monolayer).

The spectral data presented in Fig. 2 show that, at coverage of about 0.5% of a monolayer, no significant amounts of stable pairs are observed (spectrum A). As the surface coverage is increased to 1.7% (B), 3.2% (C) and 8.8% (D) of a monolayer, a red-shifted spectral broadening accompanied by the appearance of a new band at 390 nm, which results from ground state pairing, is observed. The pairing phenomenon which takes place at coverages of more than 1% of a monolayer is not observed in solutions even at very high concentrations.

The fluorescence of **1** on dry surfaces also exhibits a change in structure due to this pairing process. Fig. 3 shows the changes in the emission and excitation spectra of **1** on silica as a function of surface coverage. It can be seen from the spectral data that, at 0.5% of a monolayer, both the emission and excitation spectra (A) resemble the monomer. As the surface coverage is increased above 1% of a monolayer, monomer emission is gradually replaced by a new emission ($\lambda_{max}=420$ nm) resulting from the formation of these pairs (spectra B and C for 3.2% and 6.4% of a monolayer respectively). Comparison of the emission intensities at 382 nm (the first emission band of **1**) for 0.5% (spectrum A, Fig. 3) and 6.4% (spectrum C, Fig. 3) surface coverages

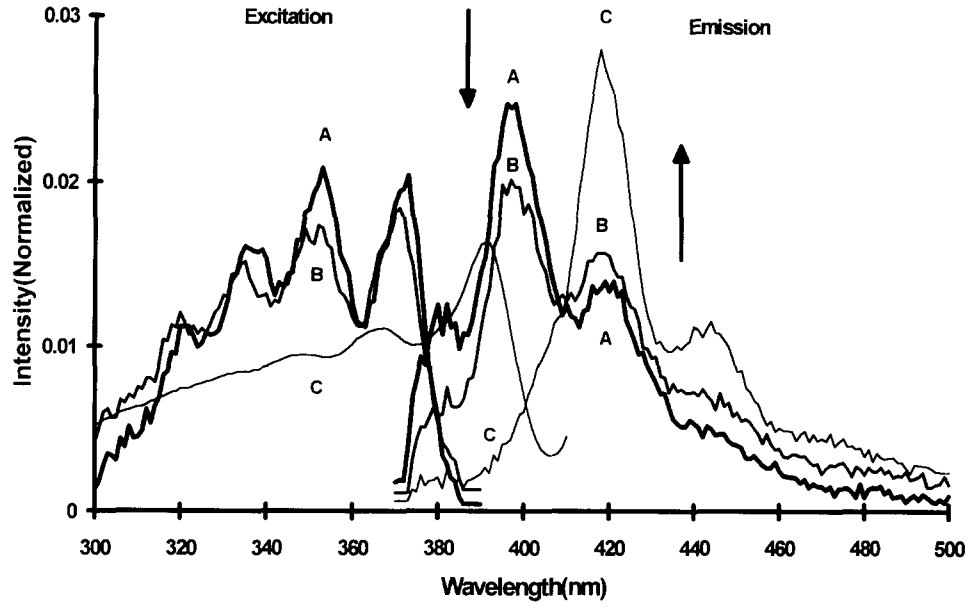

Fig. 3. Variation in the excitation ($\lambda_{em}=400$ nm for A and B and $\lambda_{em}=420$ nm for C) and emission ($\lambda_{ex}=360$ nm) spectra of **1** on dry silica (N_2 atmosphere) as a function of surface coverage: A (0.5%), B (3.2%) and C (6.4% of a monolayer). Spectra were normalized relative to the total area.

shows that about 80% of the monomer is in the stable pair form in C (this is the lower limit since calculation assumes that the stable pairs do not emit at this wavelength). Accordingly, the excitation spectra at higher coverages (C) resemble the diffuse reflectance spectra of the stable pair. A similar behavior is also observed on Cab-O-Sil and alumina.

During the course of this investigation, we noticed that pairing takes place as the solvent is evaporated from the surface. An increase in the local concentration of substrate as the solvent is removed can enhance the pairing of **1** molecules in the liquid phase with those already adsorbed on the surface active sites.

Experimental support for the role of the solvent in this process was provided by showing that the fluorescence of a freshly adsorbed sample of **1** on silica (1×10^{-4} mol g^{-1}; 10% of a monolayer), which was slightly wet due to incomplete removal of the solvent, contained monomer emission only (Fig. 4(A)). As the solvent was removed under vacuum, the monomer emission was replaced by the emission of stable pairs (Fig. 4(B)). Re-introduction of the solvent vapor restored a significant portion of the monomer emission (Fig. 4(C)).

3.1. Photodecomposition of 1 on dry surfaces

The photolysis of **1** on silica, Cab-O-Sil and alumina under deaerated conditions leads to the formation of anthracene-9,10-photodimer (**2**) as the only product. When the photolysis is carried out under an atmosphere of air, **1** undergoes photo-oxidation (major) as well as photodimerization (minor) to give the products shown in Scheme 1. Identification of the products was performed by HPLC and comparison with authentic samples. Table 1 shows the yield of photoproducts on silica and Cab-O-Sil for a typical run. The results indicate that, except for **8**, which was first observed from the photolysis of **1** in water under oxygen-deficient conditions [17], the photo-oxidation products observed on these surfaces are identical to those reported in cyclohexane slurries [14]. The major oxidation product is anthracene-9,10-endoperoxide (**3**) which undergoes a slow thermal decomposition to give 9,10-anthraquinone (**4**), 9,10-dihydro-9,10-dihydroxyanthracene (**5**), bianthronyl (**6**), 9-hydroxyanthrone (**7**) and 10,10′-dihydroxy-9,9′,10,10′-tetrahydro-9,9′-bianthryl (**8**) as the secondary products (Scheme 2). Control experiments revealed that **4** and **5** are the major decomposition products of **3**, while **6**, **7** and **8** are the minor products.

When samples containing similar surface coverages of **1** (2.5×10^{-5} mol g^{-1}) on silica, Cab-O-Sil and alumina were photolyzed at 350 nm in parallel for 15 min in the Rayonet, both silica and Cab-O-Sil showed about 73% loss of **1** compared with only 5% loss on the alumina surface. This difference in reactivity may be attributed to the much slower rate of oxygen quenching of anthracene triplets on alumina compared with silica, similar to that reported for pyrene triplets [22].

Table 2 shows the dependence of the product yields on the surface coverage for silica. An increase in the surface coverage is accompanied by an increase in the yield of dimer as well as oxidation products for coverage of up to about 5% of a monolayer. No significant change (within experimental error) in the yield of product is observed between 5% and 11% of a monolayer. The ratio of the total moles of dimeric (**2**+**6**+**8**) to mon-

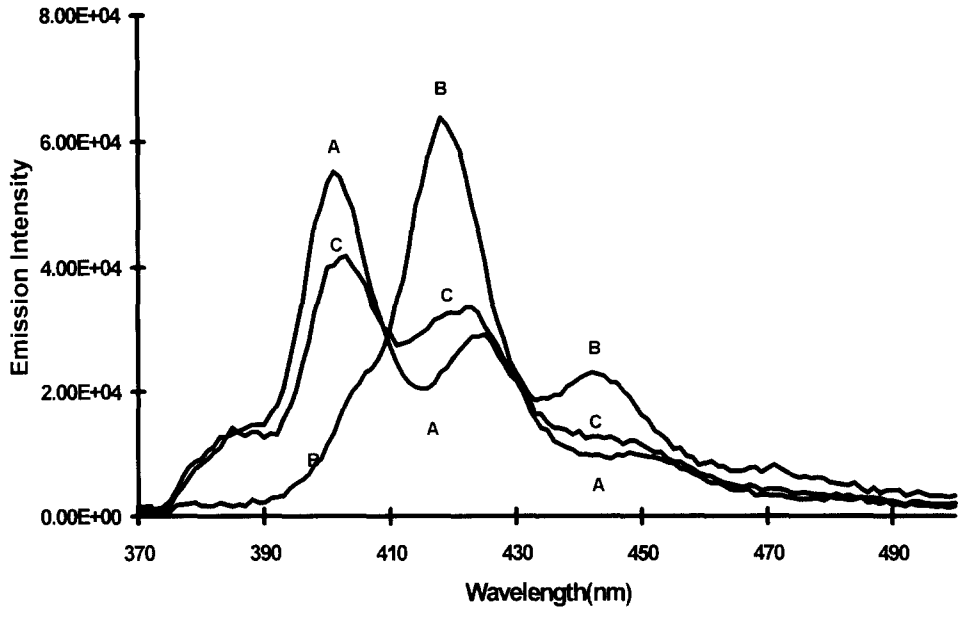

Fig. 4. Changes in the fluorescence of **1** on SiO_2 due to the formation of stable pairs as the solvent (cyclohexane) is removed: spectrum A (wet): B (solvent removed); C (solvent vapor reintroduced). N_2 atmosphere, $\lambda_{ex}=360$ nm, 1×10^{-4} mol g^{-1} (10% of a monolayer).

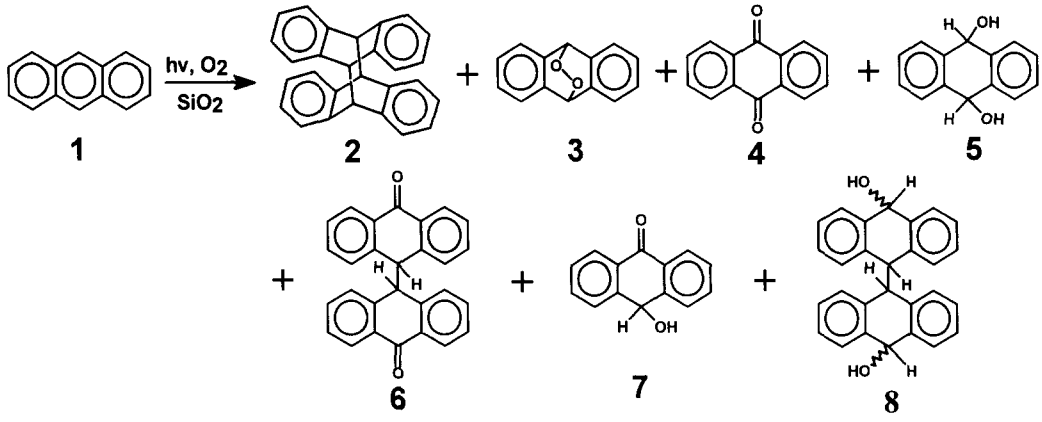

Scheme 1.

Table 1
Photoproduct yields from photolysis of anthracene on dry silica and Cab-O-Sil [a]

Surface	Loss of **1** (%)	Photoproduct (mol.%)						
		2	**3**	**4**	**5**	**6**	**7**	**8**
Silica-60	73	18	29	15	15	8	8	7
Cab-O-Sil	73	27	23	12	15	9	7	7

[a] Samples (4 g) of **1**–SiO_2 (2.5×10^{-5} mol g^{-1}; 3.7% of a monolayer) and **1**–Cab-O-Sil (2.5×10^{-5} mol g^{-1}; 4.3% of a monolayer) were irradiated at 350 nm for 15 min under an atmosphere of air (photon flux, 6×10^{16} photons cm^{-2} s^{-1}; experimental error, ±5%).

omeric (**3**+**4**+**5**+**7**) oxidation products increases linearly as a function of surface coverage up to about 5% of a monolayer and levels off at higher coverages (Fig. 5). At very low surface coverages, where the concentration of the monomeric form of **1** is significant, photolysis gives mainly photo-oxidation products and very little dimer (Table 2). As the surface coverage increases from 0.25% to 4.7%, the yield of dimeric products goes up by a factor of 28, while the corresponding monomeric products experience a seven fold increase. The change in the yield of the photodimer **2** is even more dramatic (a factor of 36, Table 2). The increase in the yield of **2** as the surface coverage approaches 5% of a monolayer is consistent with the spectroscopic data shown in Fig. 3 and clearly points to the role of the stable pairs in photodimerization.

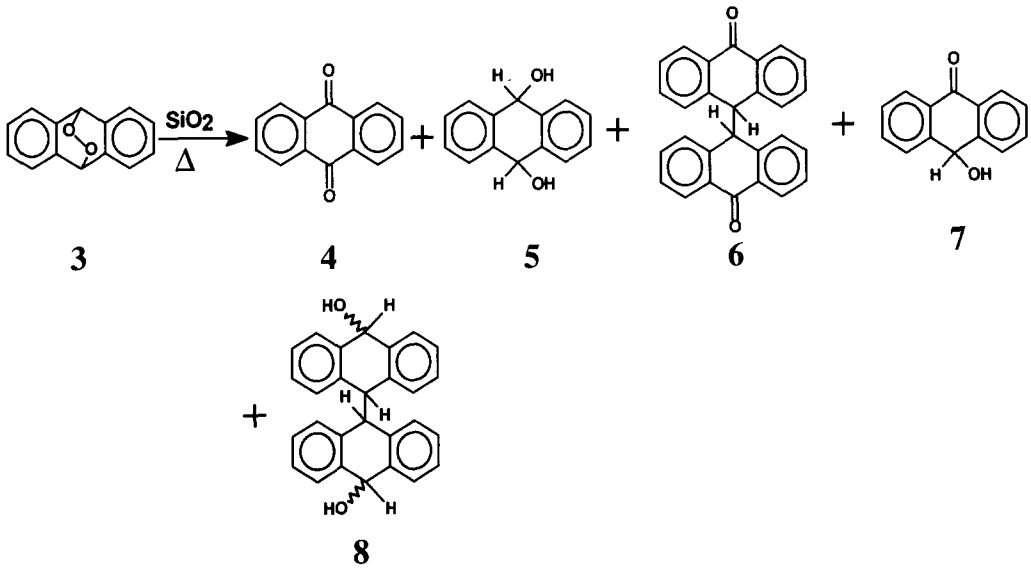

Scheme 2.

Table 2
Dependence of photoproduct yields on the surface coverage for anthracene on silica [a]

Surface coverage (%)	Moles of dimer ($\times 10^7$)	Total moles (2+6+8) ($\times 10^7$)	Total moles (3+4+5+7) ($\times 10^6$)	Total moles of oxidation ($\times 10^6$)	Ratio (2+6+8)/(3+4+5+7) (dimeric/monomeric)
0.25	0.41	0.72	0.96	1.00	0.075
0.48	0.91	1.41	1.51	1.56	0.093
0.81	1.85	2.85	1.73	1.75	0.16
1.70	5.01	6.70	4.89	5.06	0.14
2.50	8.11	11.4	6.64	6.98	0.17
3.40	9.22	12.9	6.39	6.75	0.20
3.85	8.41	12.7	7.05	7.48	0.18
4.70	14.8	20.2	6.52	7.06	0.31
6.10	15.8	21.9	7.36	7.97	0.30
6.80	16.6	23.5	7.04	7.73	0.33
7.60	14.6	21.0	6.64	7.27	0.32
9.20	15.9	22.0	6.26	6.87	0.35
9.79	13.9	19.4	7.75	8.30	0.25
10.4	11.6	16.1	6.06	6.50	0.27
10.5	15.4	22.7	8.44	9.17	0.27

[a] All samples were irradiated in a uranium glass tube at 350 nm in the Rayonet for 15 min with continuous mixing (photon flux, 6×10^{16} photons cm^{-2} s^{-1}; experimental error, ±5%).

Furthermore, we observe the same chemistry when photolysis is carried out at $\lambda_{ex}>380$ nm where stable pairs absorb strongly.

Dimerization requires diffusion of the excited singlet state of **1** on the surface to interact with a ground state molecule of **1** to form an excimer which is the precursor to **2**. At very low surface loadings, where the monomeric form of **1** is the predominant species present on the surface, dimerization by the above route is highly unlikely in view of the fact that the excited singlet state of **1** has a lifetime of about 5 ns on silica [23]. The presence of a small concentration of stable pairs on the surface can account for the observed yield of dimer at these low coverages (see below). However, due to strong overlap between the monomer and stable pair emission, a low concentration of these pairs will be difficult to detect spectroscopically because their emission will be buried under the strong monomer emission. At coverages above 5% of a monolayer, where the predominant species present on the surface are stable pairs, the absorption of the incident light (350 nm) by these pairs can lead to an excited singlet state (where the excitation is shared between the two monomers) which may re-orient to an excimer, the presumed precursor to the 9,10-photodimer (Scheme 3; SP, stable pair; EX, excimer):

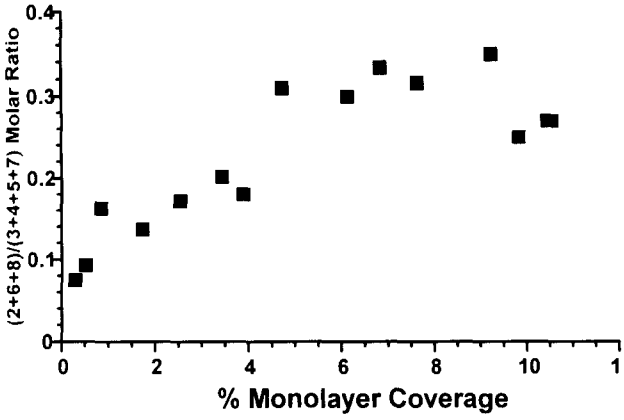

Fig. 5. Dependence of the total moles of dimeric to monomeric products (2+6+8)/(3+4+5+7)) on the surface coverage of **1** on dry silica.

$$(\mathbf{11})_{SP} \xrightarrow{h\nu} {}^1(\mathbf{11})^*_{SP} \longrightarrow {}^1(\mathbf{11})^*_{EX} \longrightarrow \mathbf{2}$$

Scheme 3.

Chandross and Ferguson [24] have reported excimer emission at 77 K from the unstable ground state sandwich pair of **1** (monomer planes and long axes are both parallel) by photodissociation of **2** in KBr. To substantiate the proposed mechanism for dimer formation (Scheme 3), a sample of **1** on silica (5% of a monolayer) was degassed in a nuclear magnetic resonance (NMR) quartz tube and photolyzed ($\lambda_{ex}=350$ nm) in the Rayonet for 1 h at room temperature. Loss of **1** with time (leading to the formation of **2**) was monitored by fluorescence spectroscopy. The tube was then immersed in a cold finger at 77 K and photolyzed at 254 nm for a total of 2 h. Under these conditions, the photodissociation of **2** leads to a ground state sandwich pair which should exhibit a structureless excimer emission at 77 K. Figure 6 shows the observed emission before (A) and after (B) the photodissociation of **2**. The structureless emission (B) with its maximum at around 470 nm is assigned to the unstable sandwich pair, which converts to the stable form on warming the sample to room temperature (spectrum C). The excitation spectrum of the sandwich pair resembles the absorption spectrum of **1** (not shown), while the excitation spectrum corresponding to the stable pair is identical to spectrum D in Fig. 2. These results clearly demonstrate that the excited unstable sandwich pair (excimer) is a possible intermediate on the reaction path from the excited stable pair to the dimer (Scheme 3). The fact that the photo-oxidation products account for the major portion of the reaction under conditions in which the concentration of the monomeric form is negligible suggests that excimer formation by the above process is not efficient. This inefficiency can be attributed to the barrier to re-orientation from the stable form to the unstable sandwich form which has the required geometry for dimerization. As a result, internal conversion, oxygen quenching and intersystem crossing into the triplet manifold can compete effectively with excimer formation (Scheme 4; SP, stable pair; EX, excimer; Re, re-orientation).

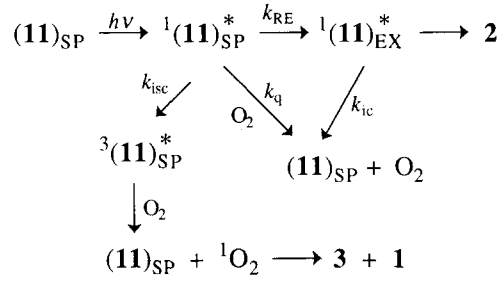

Scheme 4.

Experimental support for the role of these competing processes was provided by the following observations: (a) oxygen quenched more than 30% of the fluorescence originating from the stable pairs and (b) singlet molecular oxygen luminescence at 1270 nm (see below) was observed from the samples containing more than 5% of a monolayer on silica. These results clearly substantiate the role of stable pairs in the proposed mechanism for the photodecomposition of **1** on these surfaces.

3.2. Tests for the involvement of singlet molecular oxygen in the oxidation process

Indirect tests for the role of singlet molecular oxygen in the oxidation of **1** included: (a) the study of the sensitized reaction of **1** on SiO_2 using methylene blue (MB), a good generator of singlet oxygen on the silica surface [25], and (b) the photolysis of **1** on SiO_2 in the presence of 2,5-dimethylfuran (DMF), a well-known singlet oxygen trap [26] coadsorbed on the surface. When a 10:1 mixtures of MB–SiO_2 (1×10^{-5} mol g^{-1}) and **1**–SiO_2 (2.5×10^{-5} mol g^{-1}) was photolyzed at $\lambda_{ex}>460$ nm, where **1** does not absorb, no photodimer (**2**) was observed. Product analysis revealed that all the oxidation products shown in Scheme 2 were present. Direct photolysis ($\lambda_{ex}=350$ nm) of **1**–SiO_2 (2.5×10^{-5} mol g^{-1}) in the presence of DMF–SiO_2 (5×10^{-4} mol g^{-1}) in a 1:1 ratio led to the formation of **2** and oxidized DMF. No photo-oxidation products of **1** were observed in the presence of DMF. These results, in addition to the direct detection of singlet molecular oxygen luminescence at 1270 nm (Fig. 7) from samples of **1**–SiO_2, unequivocally implicate the role of this intermediate in inducing the oxidation of **1**.

Electron paramagnetic resonance (EPR) analysis of photolyzed samples of **1** adsorbed on silica, Cab-O-Sil or alumina showed no signal due to superoxide formation on these surfaces. We have previously detected superoxide formation on a dry silica surface from photolyzed samples of naphthalene [15]. Thus the oxidation

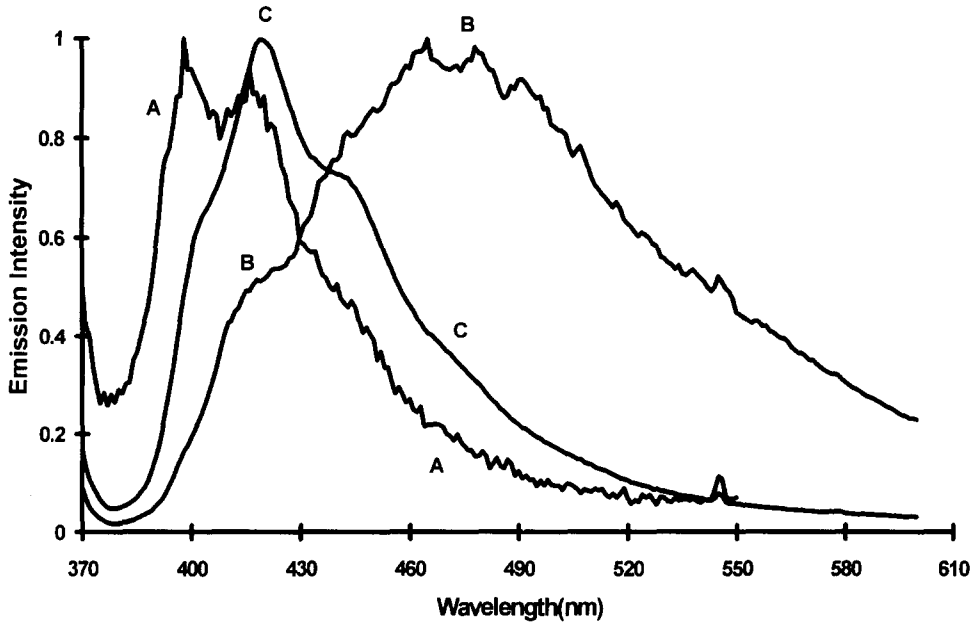

Fig. 6. (A) Normalized emission of a partially dimerized degassed sample of **1** on SiO_2 at room temperature; (B) emission at 77 K of the same sample after photolyzing at 254 nm for 2 h at 77 K; (C) emission of the photolyzed sample in B after allowing it to warm to room temperature, $\lambda_{ex} = 360$ nm.

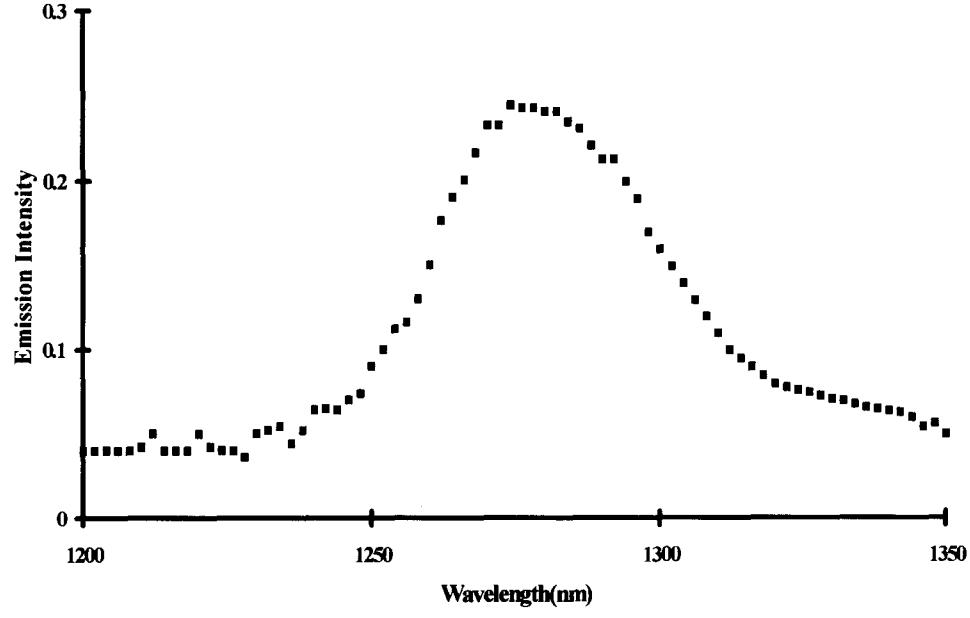

Fig. 7. Singlet oxygen luminescence of **1** on dry silica (2.5×10^{-5} mol g^{-1}, 2.5% of a monolayer, $\lambda_{ex} > 300$ nm; one scan).

of **1** proceeds by the addition of singlet oxygen to the 9,10-position of anthracene to give anthracene-9,10-endoperoxide (**3**) which undergoes thermal decomposition on the surface to produce the products shown in Scheme 2.

4. Conclusions

The photolysis of anthracene on dry surfaces of silica, Cab-O-Sil and alumina under deaerated conditions has been shown to produce the anthracene-9,10-photodimer as the only product. Irradiation in an atmosphere of air leads to the formation of the dimer (minor) and the photo-oxidation product anthracene-9,10-endoperoxide (major). The endoperoxide undergoes thermal decomposition to produce several secondary oxidation products. The photodecomposition of anthracene proceeds rapidly on the surface of silica and Cab-O-Sil but much less efficiently on alumina. The precursor to the anthracene dimer is a ground state stable pair which is observed spectroscopically at coverages of more

than 1% of a monolayer. At 5% coverage and higher, the predominant species present on the surface are stable pairs which, on excitation, lead to dimerization and photo-oxidation. The observed inefficiency of dimer formation at coverages at which the stable pairs are the predominant species present on the surface can be attributed to the barrier to re-orientation of the stable pair (in the excited singlet state) to the corresponding unstable sandwich pair which has the right geometry for dimerization. The presence of this barrier to re-orientation allows oxygen quenching and intersystem crossing into the triplet state to compete effectively with the formation of the intermediate (excimer) leading to the dimer. The photo-oxidation of anthracene is mediated by the addition of singlet molecular oxygen to ground state anthracene.

Acknowledgments

This research was sponsored by the Division of Chemical Sciences, Office of Basic Energy Sciences, US Department of Energy under contract DE-AC05-84OR21400 with Martin Marietta Energy Systems Inc. The authors also wish to thank Professor R.M. Pagni of the University of Tennessee for performing the BET surface area measurement on neutral alumina.

References

[1] O. Hutzinger (ed.), *The Handbook of Environmental Chemistry*, Vol 2, Part B, Springer, Berlin, 1982.
[2] O.C. Zafiriou, J. Joussot-Dubien, R.G. Zepp and R.G. Zika, *Environ. Sci. Technol., 18* (1984) 358.
[3] R.G. Zika and W.J. Copper, *Photochemistry of Environmental Aquatic Systems, ACS Symposium Series No. 327*, ACS, 1987.
[4] W. Stumm (ed.), *Aquatic Surface Chemistry*, Wiley, New York, 1987.
[5] G.D. Parfitt and C.H. Rochester (eds.), *Adsorption from Solution at the Solid/Liquid Interface*, Academic Press, London, 1983.
[6] P. de Mayo, *Pure Appl. Chem., 54* (1982) 1623.
[7] P. de Mayo, L.V. Natarajan and W.R. Ware, in M.A. Fox (ed.), *Organic Phototransformation in Nonhomogeneous Media, ACS Symposium Series No. 278*, ACS, 1985, pp. 1–119.
[8] J.K. Thomas, *J. Phys. Chem., 91* (1987) 267.
[9] G. Beck and J.K. Thomas, *Chem. Phys. Lett., 94* (1983) 553.
[10] S.L. Suib and A. Kostapapas, *J. Am. Chem. Soc., 106* (1984) 7705.
[11] B.H. Baretz and N.J. Turro, *J. Photochem., 24* (1984) 201.
[12] G. Chandrasekaran and J.K. Thomas, *J. Colloid Interface Sci., 100* (1984) 116.
[13] R.A. Dellaguardia and J.K. Thomas, *J. Phys. Chem., 88* (1984) 964.
[14] S.P. Zingg and M.E. Sigman, *Photochem. Photobiol., 57* (1993) 453.
[15] J.T. Barbas, M.E. Sigman, A.C. Buchanan III and E.A. Chevis, *Photochem. Photobiol., 58* (1993) 155.
[16] J.T. Barbas, R. Dabestani and M.E. Sigman, *J. Photochem. Photobiol. A: Chem., 80* (1994) 103.
[17] M.E. Sigman, S.P. Zingg, R.M. Pagni and J.H. Burns, *Tetrahedron Lett., 32* (1991) 5737.
[18] J. Ferguson, A.W.-H. Mau and J.M. Morris, *Aust. J. Chem., 26* (1973) 91.
[19] J. Ferguson, A.W.-H. Mau and J.M. Morris, *Aust. J. Chem., 26* (1973) 103.
[20] J. Ferguson, *Chem. Rev., 86* (1986) 957.
[21] W.E. Ford and P.V. Kamat, *J. Phys. Chem., 93* (1989) 6423.
[22] J.K. Thomas, *Chem. Rev., 93* (1993) 301.
[23] R.K. Bauer, R. Borenstein, P. de Mayo, K. Okada, M. Rafalska, W.R. Ware and K.C. Wu, *J. Am. Chem. Soc., 104* (1982) 4635.
[24] E.A. Chandross and J. Ferguson, *J. Chem. Phys., 45* (1966) 3564.
[25] D. Brkic', P. Frozatti, I. Pasquoss and F. Trifiro', *J. Mol. Catal., 3* (1977) 173.
[26] K. Gollnick and A. Griesbeck, *Photochem. Photobiol., 41* (1985) 2057.